European Journal of Control ∎ (∎∎∎∎) ∎∎∎–∎∎∎

Contents lists available at SciVerse ScienceDirect

European Journal of Control

journal homepage: www.elsevier.com/locate/ejcon

Structural monitoring of a tower by means of MEMS-based sensing and enhanced autoregressive models

Roberto Guidorzi [a,*], Roberto Diversi [a], Loris Vincenzi [b], Claudio Mazzotti [c], Vittorio Simioli [d]

[a] DEI, University of Bologna, viale Risorgimento 2, 40136 Bologna, Italy
[b] DIMEC, University of Modena e Reggio Emilia, via Vignolese 905, 41125 Modena, Italy
[c] DICAM, University of Bologna, viale Risorgimento 2, 40136 Bologna, Italy
[d] TELECO SpA, Via E. Majorana 49, 48022 Lugo (RA), Italy

ARTICLE INFO

Article history:
Received 9 March 2012
Accepted 24 June 2013
Recommended by A. Alessandro

Keywords:
SHM systems
Multivariate identification
AR models
AR+noise models

ABSTRACT

Structural Health Monitoring (SHM) methodologies are taking advantage of the development of new families of MEMS sensors and of the available network technologies. Advanced systems rely on intelligent bus-connected sensing units performing locally data filtering, elaboration and model identification. This paper describes a family of enhanced multivariate autoregressive models that can be used in SHM-oriented identification procedures and the implementation of a new advanced SHM system in the tower of the Engineering School of Bologna University. It describes also the results given by the considered procedure and a comparison of the implemented MEMS-based system with a traditional solution based on piezoelectric seismic accelerometers.

1. Introduction

Civil infrastructures, like highways, bridges, airports, seaports, railroads, water management systems, oil and gas pipelines, are of paramount importance for economic and industrial development. These systems are characterized by high costs, strong impact on the safety and quality of life for large communities and long operative lives. Their proper management requires, consequently, the adoption of carefully selected policies developed taking into account the delicate balance between potentially conflicting requirements like, for instance, achieving high safety standards and limiting maintenance costs [1]. Moreover, some specific events like earthquakes, floods or tornadoes can lead to very critical decisions in ascertaining the integrity of surviving structures and their suitability to fulfill their intended role [30]. Similar problems afflict the evaluation of the state of structures built during the last century (e.g. many bridges in the United States) and of ancient buildings inside large cities, exposed to the stress caused by the increase of surface and underground urban transport systems. The relevance of these problems is not limited, however, to the evaluation of the state of structures potentially damaged by traumatic events; the advanced technologies implemented in the realization of new projects, for instance, buildings with active seismic response control systems [31,13] are even more demanding since they require a proper monitoring concerning the whole operating life of the structures.

Structural identification is, in general, considered as an applied methodology for characterizing a structural system using measurements describing how the structure behaves under loading [3,33]. Structural Health Monitoring (SHM) relies on structural identification techniques to perform comparisons between the reference dynamical behavior of the monitored structures and the current one [5,38,10]. Due to the large number of uncertainties and the unavoidable simplifications performed during the modeling processes (see for instance wind or seismic loading conditions, behavior of materials and the contributions of non-structural elements) the real structural behavior is always different from the descriptions obtained with structural models; it is thus appropriate to verify that the real structural performances match with the model response [32]. In addition, the structural system can be subjected to changes (damages) of the material/geometric properties, including changes of the boundary conditions and system connectivity, which adversely affect the system's performance [10]. The SHM process involves the observation of a system over time using periodically sampled dynamic response measurements from an array of sensors with a suitable sampling rate. Traditional SHM systems are essentially composed of a certain number of analog sensors (strain gauges, accelerometers, temperature sensors) connected, through signal conditioning units, to multichannel data loggers. The measures obtained from these sensors are the structure response to external or internal

* Corresponding author. Tel.: +39 0512093027
E-mail addresses: roberto.guidorzi@unibo.it (R. Guidorzi), roberto.diversi@unibo.it (R. Diversi), loris.vincenzi@unimore.it (L. Vincenzi), claudio.mazzotti@unibo.it (C. Mazzotti), vsimioli@telecogroup.com (V. Simioli).

0947-3580/$ - see front matter © 2013 European Control Association. Published by Elsevier Ltd. All rights reserved.
http://dx.doi.org/10.1016/j.ejcon.2013.06.004

excitations due to wind and other meteorological phenomena, vehicle traffic, seismic events, mass movements [36] or use of specific excitation hardware like mechanical shakers [26]. The evaluation of the information contained in the data is then usually performed off-line by experts relying on suitable models of the structure to be analyzed and on the compliance of these models with the measured data. Damage-sensitive features and the statistical analysis of these features are then used to determine the current state of the system health. The application of SHM techniques leads to a periodically updated information regarding the ability of the structure to perform its intended function in the presence of the inevitable aging and degradation resulting from operational environments. After extreme events, such as earthquakes, SHM is used for rapid condition screening and aims to provide, in near real time, reliable information regarding the integrity of the structure [30]. The state of the structure can be evaluated by comparing the responses obtained in reference (integrity) conditions with the current ones [10,9]; these comparisons could be (and, sometimes, are) performed by directly extracting from the collected time series information depending only on the structure [11,29,22,39]. In other words, Structural Health Monitoring aims to give, at every moment during the life of a structure, a diagnosis of the "state" of the different parts, and of the full assembly of these parts constituting the structure as a whole. The state of the structure must remain in the designed range despite the deterioration due to usage, the action of the environment and accidental events.

In this complex and demanding context, SHM methodologies are taking advantage of the unprecedented development of sensors, microelectronics and microprocessor technologies [6,28], wireless communications [25,21,37,23], and are moving towards their life-long integration in new projects while still playing the role of advanced analysis tools for evaluating the state of structures not endowed with permanent monitoring systems. In particular, the introduction of MEMS sensors [6] allows the realization of systems that conjugate a reduced cost with performances suitable for SHM applications. The new generation of SHM systems relies on designs that integrate advanced sensor technologies with distributed computational power as well as efficient implementations of identification methodologies. These advanced systems rely on intelligent sensors that elaborate local models and exchange data, information and models on a local network under the supervision of a control/storage unit accessible also in the Internet.

The purpose of this paper is twofold. A first contribution concerns the use of AR+noise models [7] in applications that fit their stochastic environment like in the case of this application. A second contribution concerns the description of the practical results given by a new SHM system developed at Bologna University and engineered by Teleco SpA whose advanced architecture, based on a digital bus and on MEMS sensors, is basically different from traditional ones based on radial analog connections of piezoelectric sensors. The data sets used for identification and validation purposes have been collected on the experimental system installed in the Tower of the School of Engineering of Bologna University during small seismic events. Further data have been collected from temporarily installed traditional piezoelectric accelerometers and have been used for a comparative analysis.

2. Modeling data in SHM applications

All dynamic SHM implementations rely on data, measured with a suitable sampling rate, acquired by a certain number of accelerometers mounted on the structure to be monitored. SHM systems usually generate enormous amounts of data that must be processed and stored. To avoid the off-line manipulation of all data, it is preferable to implement automated procedures [30,14,27] or to work only on some form of concentrated information extracted from the data, like dynamic models obtained by means of identification techniques. These techniques allow not only for a very large condensation of information but can also be effectively used to separate the information contained in the acquired data sets from the observation errors due to the intrinsic noise of the sensors and to the inevitable misfit between the considered class of models and the real process to be described. Thus the power spectrum associated with an identified model will look as (and will be) a smoothed version of that directly obtained by applying FFT techniques to the measured sequences that would also lead to many spurious lines due to the additive noise.

In typical SHM applications, the process input, i.e. the excitation applied to the structure, is only seldom measured (usually this happens only when artificial inputs are applied for test purposes by means of hammers, mechanical shakers or other methods); in almost all permanent implementations of SHM systems the excitation is given by vehicle traffic or natural phenomena as seismic events and wind pressure and is not directly measured. The available data are thus given by sequences of observations, $y(1), y(2), \ldots, y(L)$, where $y(t)$ denotes the vector of acceleration measures, i.e.

$$y(t) = [y_1(t)\ y_2(t)\ \ldots\ y_m(t)]^T. \tag{1}$$

A class of models frequently used to represent observations of this kind is given by multivariate AR processes, described by the relation

$$y(t) = Q_1 y(t-1) + Q_2 y(t-2) + \cdots + Q_\mu y(t-\mu) + e(t) \tag{2}$$

where the matrices Q_i $(i = 1, \ldots, \mu)$ are square $(m \times m)$ coefficient matrices,

$$Q_i = \begin{bmatrix} q_{11i} & q_{12i} & \cdots & q_{1mi} \\ q_{21i} & q_{22i} & \cdots & q_{2mi} \\ \vdots & \vdots & \ldots & \vdots \\ q_{m1i} & q_{m2i} & \cdots & q_{mmi} \end{bmatrix}, \tag{3}$$

the integer μ denotes the memory of the model and

$$e(t) = [e_1(t)\ e_2(t)\ \ldots\ e_m(t)]^T \tag{4}$$

is a vector whose elements $e_i(t)$ $(i = 1, \ldots, m)$ are white processes with null expected value, $\mathrm{E}[e_i(t)] = 0$, and with variances σ_{ei}^2; these processes can be mutually correlated so that the covariance matrix of $e(t)$ is not necessarily diagonal. By denoting with z^{-1} the unitary delay operator, model (2) can also be written in the compact polynomial form:

$$Q(z^{-1})y(t) = e(t) \tag{5}$$

where $Q(z^{-1})$ is the polynomial matrix

$$Q(z^{-1}) = I - Q_1 z^{-1} - \cdots - Q_\mu z^{-\mu}. \tag{6}$$

Fig. 1 shows a possible interpretation of multivariate AR models that can be seen as filters driven by the input vector $e(t)$ with transfer matrix $Q(z^{-1})^{-1}$ and output vector $y(t)$.

Model (2) belongs to the family of equation error models and its optimal predictor (minimal variance and whiteness of the prediction error on every output) is given by [17]

$$\hat{y}(t) = Q_1 y(t-1) + Q_2 y(t-2) + \cdots + Q_\mu\, y(t-\mu) \tag{7}$$

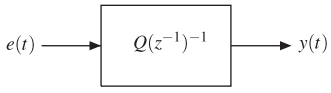

Fig. 1. Interpretation of multivariate AR models.

Please cite this article as: R. Guidorzi, et al., Structural monitoring of a tower by means of MEMS-based sensing and enhanced autoregressive models, European Journal of Control (2013), http://dx.doi.org/10.1016/j.ejcon.2013.06.004

and its prediction error $\varepsilon(t)=y(t)-\hat{y}(t)=e(t)$ coincides with the equation error. By denoting with θ a generic set of parameters of the model, i.e. a generic set of entries of the matrices Q_i, the prediction error obtained by using this parameterization in predictor (7) will be denoted as $\varepsilon(t,\theta)=y(t)-\hat{y}(t,\theta)$; it coincides with $e(t)$ only when the entries of θ are the exact parameters, θ^*, of the AR process that has generated the data. The model parameters are usually estimated by minimizing the Euclidean norm of the prediction error $\varepsilon(t,\theta)$:

$$J(\theta)=\frac{1}{N}\sum_{t=\mu+1}^{L}\|\varepsilon(t,\theta)\|_2^2=\frac{1}{N}\sum_{t=\mu+1}^{L}\varepsilon(t,\theta)^T\varepsilon(t,\theta)=\frac{1}{N}\sum_{i=1}^{m}\sum_{t=\mu+1}^{L}\varepsilon_i(t,\theta_i)^2 \tag{8}$$

where $N=L-\mu$, θ_i is the vector of the coefficients appearing in the i-th row of $Q(z^{-1})$

$$\theta_i=[q_{i11}\ldots q_{im1}\ldots q_{i1\mu}\ldots q_{im\mu}]^T, \tag{9}$$

and $\varepsilon_i(t,\theta)=y_i(t)-\hat{y}_i(t,\theta)$. The minimization of $J(\theta)$ can be easily performed by means of the Least Squares (LS) method [17]. For this purpose, define the Hankel matrix of output samples

$$H(y_i)=\begin{bmatrix} y_i(1) & y_i(2) & \ldots & y_i(\mu) \\ y_i(2) & y_i(3) & \ldots & y_i(\mu+1) \\ \vdots & \vdots & \ldots & \vdots \\ y_i(N) & y_i(N+1) & \ldots & y_i(L-1) \end{bmatrix}, \tag{10}$$

the matrix

$$H=[H(y_1)\ H(y_2)\ \ldots\ H(y_m)] \tag{11}$$

and the vector of output samples

$$y_i^o=[y_i(\mu+1)y_i(\mu+2)\ldots y_i(L)]^T. \tag{12}$$

Then, under suitable excitation conditions (non-singularity of (H^TH)), the LS estimate of θ_i is given by

$$\hat{\theta}_i=(H^TH)^{-1}H^Ty_i^o \quad (i=1,\ldots,m). \tag{13}$$

All previous steps can be easily performed on the basis of a set of observed process sequences but requires a previous choice of the model memory, μ (the model order is $n=\deg\det Q(z^{-1})=m\mu$). Of course, when the observations are generated by a true multivariate AR process, μ and n should assume their true values and could be estimated by applying suitable order selection criteria like FPE (Final Prediction Error), AIC (Akaike Information Criterion), MDL (Minimum Description Length) or others [17,24]. These criteria are usually formulated for the univariate case but can be easily extended to the multivariate one. While all previous criteria give correct results for data generated by true AR processes, real processes are intrinsically distributed so that the correct model memory should be infinite and different criteria can lead to different evaluations.

A reliable criterion that can be applied in the identification of real processes and that can be used not only to select a proper model order but also to validate the whole identification procedure consists in checking the whiteness of the prediction errors $\varepsilon_i(t,\theta)$; this happens only if the model order is sufficient and the description of the considered process by means of an AR model is acceptable. A good strategy can thus consist in starting with $\mu=1$ and increasing μ checking, at every step, the whiteness of the sequences $\varepsilon_i(t,\theta)$; as soon as all these sequences satisfy a proper whiteness test (for instance a χ^2 test with a number of degrees of freedom equal to 2–3 times the model memory and a confidence level of, say, 99%), a suitable model memory has been reached. It must, however, be observed that the use of higher values, while leading to overparameterized models and to higher uncertainty levels for the parameters, does not lead, usually, to a crash of the identification procedure or to worse results and this can be easily explained by the previous observation on the nature of real processes.

The choice of the algorithms to estimate the parameters of multivariate AR models is not limited to Least Squares; another possibility concerns the use of Yule–Walker equations or of the wide class of Instrumental Variable (IV) algorithms (in fact Yule–Walker equations constitute a subcase of the IV approach where past outputs are used as instruments). These options can be used to compensate a possible lack of whiteness in the equation error sequences (by avoiding the use of the first low order equations when using Yule–Walker equations, by selecting suitable instruments when relying on IV approaches) but lead, in general, to a larger uncertainty on the parameter estimates, i.e. to covariance matrices of the estimates larger than the LS one. Other possibilities concern the use of on-line algorithms, typically on-line least squares (weighted or not) to update a model as long as new measures are performed. The Levinson algorithm offers an elegant and efficient way to compute increasing-order AR models from data covariances. A sequence of increasing-order AR models can also be estimated directly from the data by means of least squares approaches.

It has been shown that reliable procedures for modal identification can be used to develop an efficient modal-based Structural Health Monitoring system using, for example, the AR (or ARX) coefficients as damage-sensitive parameters [11,29,34]. Moreover, unlike other dynamic models, AR models are unaffected by overparameterization. When these algorithms are applied to records, including the structural response to a ground motion, they can lead to unreliable results due to the fact that the hypothesis about the input (white noise) could not be fulfilled by the earthquake spectra. It is worth noting that the near-fault ground motion spectra are significantly different from those obtained in a far-field condition [2] in that usually a near-fault earthquake can be viewed as an impulse; moreover, intensity, ground motion spatial variations and local site conditions can influence significantly the earthquake spectra. For these reasons, in some cases the ground motion spectra can be assumed as flat at least in the range of frequencies of interest. In these cases, the input of the process to be identified can be assumed as white.

Once that a multivariate AR model has been identified, it is also possible to obtain equivalent representations to fulfill specific needs; control applications could call, for instance, for state-space models. Other representations frequently used are the transfer matrix between the driving noise and the output, $Q(z^{-1})^{-1}$, the impulse response (AR models do not consider any measurable input; the input pulse is considered on the components of $e(t)$) and the model power spectra. When the models must be used for fault diagnosis applications, as in SHM, the choice of the representation to be used can be critical. Consider, as an example, a non-minimally parameterized model; its parameters could exhibit large but mutually compensated variations also in the absence of significant process changes. It is thus important to observe possible changes, to look at model properties reflecting actual variations of the identified process; possible choices could concern the parameters of minimally parameterized models, model poles, frequency responses, power spectra and cross-spectra.

Another desirable feature usually absent in identified models concerns the physical significance of the models; the models obtained by means of identification techniques can be very accurate but usually lack, differently from those obtained by means of traditional modeling techniques, a direct physical meaning. This requirement and the previous one lead often to the use, in SHM applications, of the spectra and cross-spectra associated with the identified multivariate models. This information reflects well defined physical properties of the structures and can be easily linked to project-level evaluations.

Please cite this article as: R. Guidorzi, et al., Structural monitoring of a tower by means of MEMS-based sensing and enhanced autoregressive models, European Journal of Control (2013), http://dx.doi.org/10.1016/j.ejcon.2013.06.004

Remark 1. Relation (2) is universally considered as the standard definition of multivariate AR models. This definition is, however, afflicted by conceptual limitations because of the implicit assumption that all channels have the same memory; thus the order of the processes described by these models can assume only values multiples of the model memory. More general and minimally parameterized representations of multivariate systems have been described in [15–17] and could also be used in the SHM context to obtain more physically precise descriptions of complex structures. Good results can usually also be obtained by using basic AR models like (2) and (5).

3. Advanced AR modeling: AR+noise representations

Traditional AR models are endowed with many advantages that range from the easy estimation of their parameters by means of unbiased and efficient algorithms like LS to the stability of the associated optimal predictors (independent from the stability of the model). These models can be interpreted according to the scheme reported in Fig. 1 where the equation error $e(t)$ is considered as input of a filter; in these models the equation error $e(t)$ is the only tool available to describe the different causes for misalignment between the model and the data (non-linearities, process noise, observation errors, non-stationarity, etc.). A more sophisticated way to manage these inevitable misalignments consists in introducing a specific description of the observation errors, separating these errors from those due to other causes. AR +noise models consist in AR models whose output is considered to be affected by an additive observation error (Fig. 2).

AR+noise models are thus described by the equations:

$$y^*(t) = Q_1 y^*(t-1) + \cdots + Q_\mu y^*(t-\mu) + e(t) \tag{14}$$

$$y(t) = y^*(t) + w(t) \tag{15}$$

where

$$w(t) = [w_1(t)\ w_2(t)\ \ldots\ w_m(t)]^T \tag{16}$$

is a vector whose elements $w_i(t)$ $(i=1,\ldots,m)$ are white processes mutually uncorrelated, uncorrelated with the entries of $e(t)$, with null expected value, $\mathrm{E}[w_i(t)]=0$, and with variances σ^2_{wi}; the covariance matrix of $w(t)$ is thus diagonal

$$\Sigma_w = \mathrm{diag}[\sigma^2_{w1}\ \sigma^2_{w2}\ldots\sigma^2_{wm}]. \tag{17}$$

More general AR+noise schemes could consider additive colored noise on the observations and/or the presence of correlations between the observation noises. The interest, in SHM implementations, of the first extension is modest while the second one, as it will be shown in the sequel, can be necessary for a realistic description of some sensors.

The identification of AR+noise models is more complex than the identification of AR models because it is necessary to estimate not only the parameters of $Q(z^{-1})$ and the covariance matrix of $e(t)$ but also the covariance matrix of $w(t)$ and, in this stochastic context, LS would lead to biased estimates.

The parameters of AR+noise models could be estimated by means of IV algorithms; the disadvantage of this solution concerns the uncertainty of the estimates and the fact that the variances of the equation errors and of the observation noise are not estimated. Another approach could rely on mapping the AR+noise identification problem into an EIV identification scheme, more precisely into the Frisch scheme that allows estimating, by means of a search procedure, both model parameters and the observation and process noise variances [18]. The estimate of AR+noise models by means of a Frisch-scheme approach has been described in [7,8] for the univariate case but can be extended to the multivariate context. An approach of this kind has the advantage of leading to a congruent solution and of being intrinsically suitable for fault diagnosis; a possible disadvantage concerns the fact that the stability of the obtained model is not assured. Another way to solve the problem could rely on the use of compensated least squares schemes, like BELS algorithms [40,41]. These algorithms are iterative and, usually, fast but they assure neither congruence nor convergence.

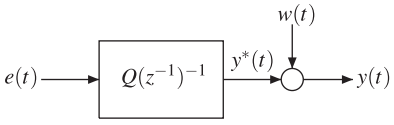

Fig. 2. Structure of AR+noise models.

An approach suggested by filtering techniques applied in speech enhancement relies on the separate estimate of the variance of the additive observation noise from sequences collected in the absence of signals (silent frames). This estimate is then used to compensate the presence of the observation noise reducing thus the AR+noise estimation problem to the estimation of an AR model. A procedure of this kind can also be adopted in the multivariate case and effectively applied in the SHM context. It allows also the extension to more general contexts where not all observation errors are independent and this can be of practical relevance in SHM. To illustrate this two-step procedure, consider, for an AR+noise process, the covariance matrix

$$\Sigma^* = \lim_{N\to\infty} \frac{H^{*T}H^*}{N} \tag{18}$$

where H^* has the same structure as H and is constructed with samples, $y^*(t)$, of the AR part of the model. Because of the relation $y(t)=y^*(t)+w(t)$ and of the assumption of non-correlation between $e(t)$ and $w(t)$, and, consequently, between $y^*(t)$ and $w(t)$, it follows that

$$\Sigma = \lim_{N\to\infty} \frac{H^TH}{N} = \Sigma^* + \Sigma_{oe} \tag{19}$$

where Σ_{oe} denotes the covariance matrix of observation errors

$$\Sigma_{oe} = \mathrm{diag}[\sigma^2_{w1}I_\mu\ldots\sigma^2_{wm}I_\mu]. \tag{20}$$

If Σ_{oe} is known, it is possible to deduce Σ^* from (19) and, consequently, to reduce the problem to the identification of an AR process by substituting H^TH with $N\Sigma$. In practical applications relation (19) will be applied to the available sample quantities by means of the relation

$$H^{*T}H^* = H^TH - N\Sigma_{oe} \tag{21}$$

and, under the assumption of non-correlation between $e(t)$ and $w(t)$, an asymptotically unbiased estimate of the AR model parameters is

$$\hat\theta_i = (H^TH - N\Sigma_{oe})^{-1}H^Ty_i^o \quad (i=1,\ldots,m). \tag{22}$$

An estimate of Σ_w and, consequently, of Σ_{oe} can be obtained by computing the sample covariance matrix of output sequences that do not contain any useful information (silent frames); this can be verified by means of a whiteness test on the components of $y(t)$.

Remark 2. The subtraction from the main diagonal of Σ of the diagonal elements of Σ_w (in blocks of μ elements) can lead to non-positive definite matrices ($H^TH - N\,\Sigma_{oe}$) and/or to estimate unstable models. The reasons derive both from the approximation associated with the use of sample quantities and from the assumption of zero off-diagonal elements in Σ_{oe}. When this happens it is possible to modify relation (22) as follows:

$$\hat\theta_i = (H^TH - kN\Sigma_{oe})^{-1}H^Ty_i^o \quad (i=1,\ldots,m) \tag{23}$$

Please cite this article as: R. Guidorzi, et al., Structural monitoring of a tower by means of MEMS-based sensing and enhanced autoregressive models, European Journal of Control (2013), http://dx.doi.org/10.1016/j.ejcon.2013.06.004

where $0<k<1$ is chosen in order to respect the condition $(H^TH-kN\Sigma_{oe})>0$ and the stability constraint.

4. The SHM system in the tower of the Engineering School of Bologna University

The building where the tower is located has been designed by the Italian architect Giuseppe Vaccaro and was built between 1933 and 1935 (Fig. 3). The tower is actually an archive capable of holding over 60,000 volumes, arranged on movable metal shelves. It is approximately 45 m high and its structure is characterized by four rectangular columns which support nine concrete slabs. The measures are performed by means of a prototype of the advanced SHM system developed at the University of Bologna and engineered by Teleco, the SHM602 [35], compliant with the recommendations reported in [12,19].

The main components of this system consist in a controller/storage unit TSD10 and in intelligent sensing units TSM02 connected to the controller by means of a serial bus. Every sensing unit can send the measures of the acceleration on two orthogonal axes and that of the temperature; the sampling frequency can be selected by the user at 20 Hz, 40 Hz or 80 Hz. These units rely on MEMS sensors that, because of the used local digital filtering techniques and oversampling rates, exhibit a noise floor almost one order of magnitude lower than that of other MEMS based systems. The dynamic behavior of the tower is monitored by means of four TSM02 units (eight accelerometers) installed in four different floors (M1–M4 in Figs. 4 and 5). Their locations have been carefully chosen in order to avoid nodal points (zero response points) on the first several vibration mode shapes. Four piezoelectric single-axis accelerometers (denoted as A1–A4 in Figs. 4 and 5) have been temporarily installed in two of the previous locations for comparison purposes. A first set of measures (in mg) has concerned the evaluation of the signal variances in the absence of excitation; this can be easily performed since the building is located in a quiet area, outside traffic patterns. The obtained sample variances and covariances are reported in Table 1 where it can be observed that the noises on the x- and y-axes of the same unit exhibit a non-negligible correlation; the covariance values associated with accelerometers of different sensors (not reported in Table 1) are, on the contrary, negligible. This observation can be easily explained since the accelerometers of every TSM02 unit are physically allocated on the same MEMS chip. It can also be observed that the obtained variances are perfectly aligned with the nominal values of TSM02 units with the exception of the fourth sensor whose noise level is approximately 20% lower.

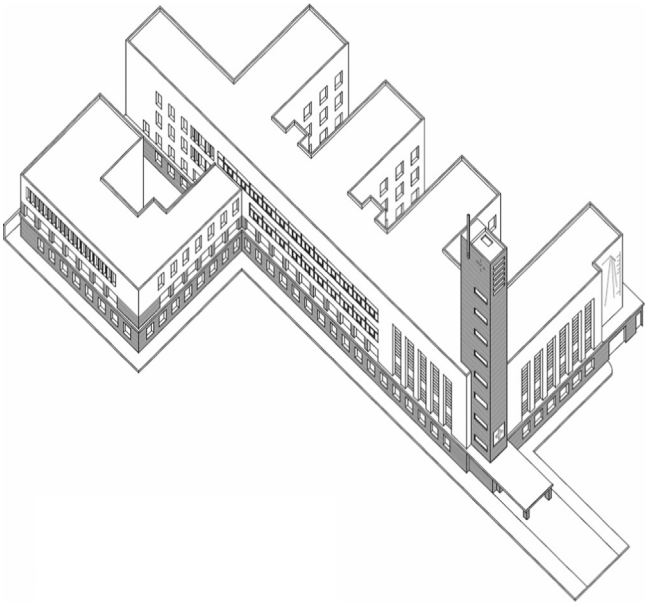

Fig. 3. The Engineering School building.

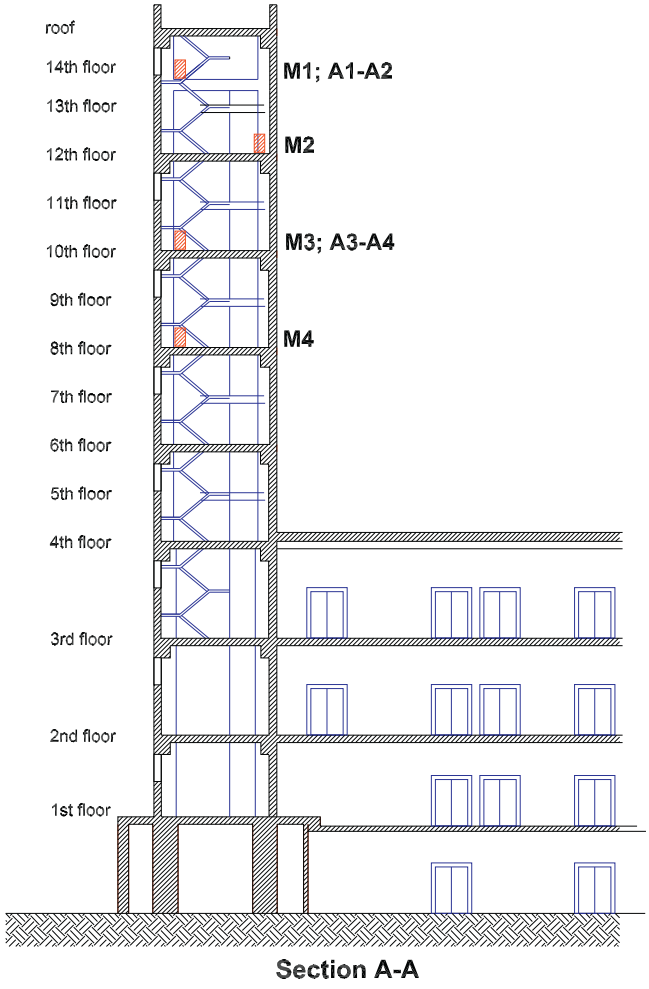

Fig. 4. Accelerometer locations in the tower.

The stochastic environment of the considered application and the possibility of constructing a sample noise covariance matrix on the basis of the measures in the absence of excitation suggest the use of AR+noise models instead of AR models. It can also be observed that, from a spectral point of view, AR+noise models are equivalent to ARMA models [20] that, however, would not allow exploiting the available information about the observation noise.

4.1. Results of the identification experiments

Several models using all eight available channels and characterized by different memory values have been tested; of course increasing the memory model leads to higher resolutions of the associated power spectra. The model described in the following is limited to four channels in order to comply with space constraints without omitting any feature of interest of the adopted procedure; its memory is $\mu=80$ in order to allow a fair comparison between the model spectrum and the spectrum directly obtained from the observations. The measures considered in the construction of this model are reported in Table 2.

The identification has been performed by using AR+noise models and the covariance matrix of the observation noise has

Please cite this article as: R. Guidorzi, et al., Structural monitoring of a tower by means of MEMS-based sensing and enhanced autoregressive models, European Journal of Control (2013), http://dx.doi.org/10.1016/j.ejcon.2013.06.004

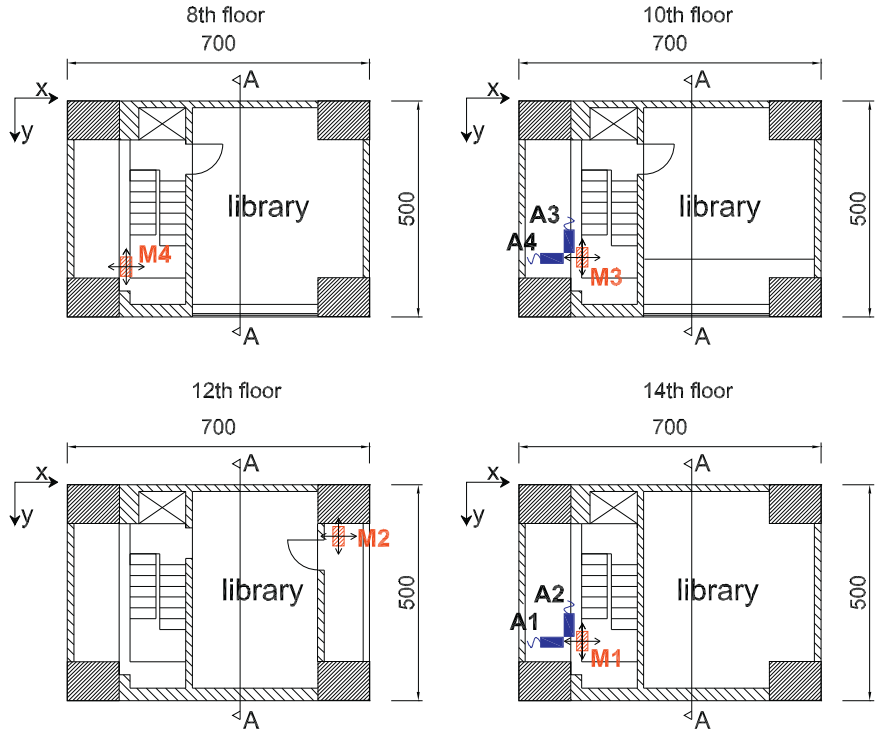

Fig. 5. Accelerometer locations in the selected floors.

Table 1
Variances and covariances of measured noise.

Sensors	σ_x^2	σ_y^2	σ_{xy}
Sensor M1	0.1087	0.0952	−0.0421
Sensor M2	0.0993	0.0986	−0.0379
Sensor M3	0.1061	0.0965	−0.0373
Sensor M4	0.0773	0.0771	−0.0315

Table 2
Model outputs.

Sensors	Channel 1 y_1	Channel 2 y_2	Channel 3 y_3	Channel 4 y_4
Sensor M1	x-axis	y-axis	–	–
Sensor M2	–	–	y-axis	–
Sensor M3	–	–	–	y-axis
Sensor M4	–	–	–	–

been constructed on the basis of the measures reported in Table 1. Since two channels of the same sensor have been inserted in the model, considering a diagonal covariance matrix Σ_w for the additive observation noise would not be congruent with the measured covariances; thus the evaluation of Σ_w that has been actually used is

$$\Sigma_w = \begin{bmatrix} 0.1087 & -0.0421 & 0 & 0 \\ -0.0421 & 0.0952 & 0 & 0 \\ 0 & 0 & 0.0986 & 0 \\ 0 & 0 & 0 & 0.0965 \end{bmatrix} \quad (24)$$

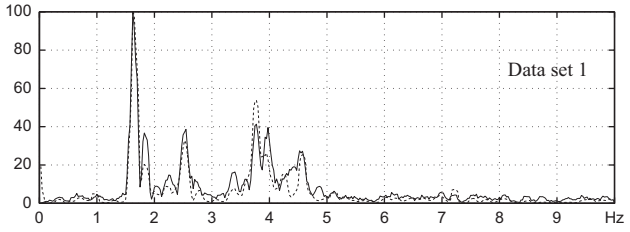

Fig. 6. Normalized power spectra of y_1; data-based (continuous line) and model-based (dashed line).

and congruent variations have been introduced in Σ_{oe} that assumes the following form:

$$\Sigma_{oe} = \begin{bmatrix} 0.1087I_\mu & -0.0421I_\mu & 0 & 0 \\ -0.0421I_\mu & 0.0952I_\mu & 0 & 0 \\ 0 & 0 & 0.0986I_\mu & 0 \\ 0 & 0 & 0 & 0.0965I_\mu \end{bmatrix}. \quad (25)$$

The data set used for the identification has been recorded on December 5, 2010 and concerns a small seismic event with magnitude 3.2 observed at a depth of 15 km in the area of Castel San Pietro Terme, at a distance of 28 km from Bologna. The most suitable k values to be used in (23) have been obtained from tests on the positive definiteness of $(H^TH - kN\Sigma_{oe})$ and on the stability of the AR+noise model. A comparison between the power spectra of the four observed sequences and those computed by means of the identified model is reported in Figs. 6–9 where the "data-based" PSDs have been obtained from the FFT of the observed signals (computed by means of the classical Cooley–Tukey algorithm). Moreover, the Matlab smooth function and a scaling normalization have been used for an easier comparison.

The significant peak frequencies obtained from these models are reported in Table 3. It can be observed that the main resonance

Please cite this article as: R. Guidorzi, et al., Structural monitoring of a tower by means of MEMS-based sensing and enhanced autoregressive models, European Journal of Control (2013), http://dx.doi.org/10.1016/j.ejcon.2013.06.004

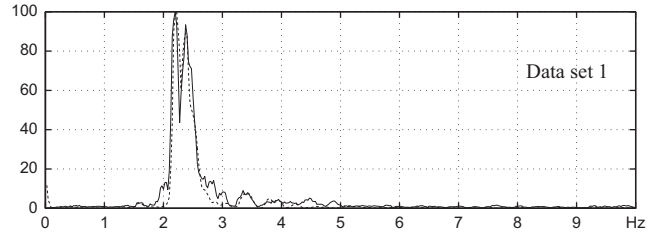

Fig. 7. Normalized power spectra of y_2; data-based (continuous line) and model-based (dashed line).

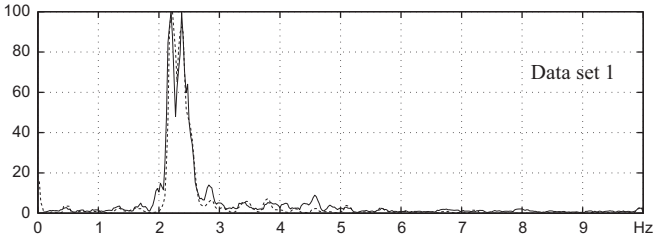

Fig. 8. Normalized power spectra of y_3; data-based (continuous line) and model-based (dashed line).

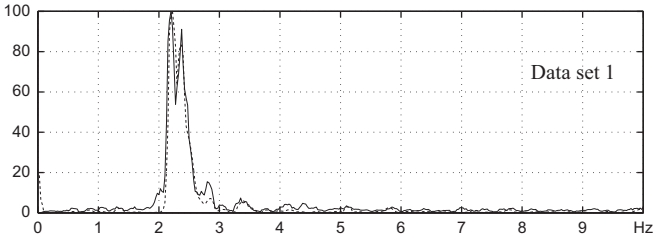

Fig. 9. Normalized power spectra of y_4; data-based (continuous line) and model-based (dashed line).

Table 3
Peak frequencies (model 1/model 2).

Channel 1	1.60/1.60	1.75/1.80	–	2.45/2.50	3.725/3.85
Channel 2	–	–	2.20/2.20	2.40/2.40	–
Channel 3	–	–	2.20/2.20	2.40/2.40	–
Channel 4	–	–	2.20/2.20	2.40/2.40	–

frequencies along the x-axis are approximately 1.60 and 1.80 Hz while a third frequency is around 3.8 Hz; the resonance frequencies along the y-axis are approximately 2.2 Hz and 2.40 Hz.

4.2. Validation of identification results

Validating a model consists, essentially, in verifying whether the model is suitable for the purpose that has suggested its construction; it is thus possible to adopt different validation criteria in different applications. In this case the most relevant information associated with the identified models concerns their PSD and, consequently, it makes sense to compare the PSDs of models obtained from different data sets because their congruence can confirm the absence of damages and the model suitability in describing the structure's behavior. A second model has thus been obtained from data recorded on December 6, 2010 concerning another small seismic event with magnitude 3.0 observed at a depth of 24 km in the same area as the previous one. The comparison between the power spectra of the four observed sequences and those computed by means of the identified model

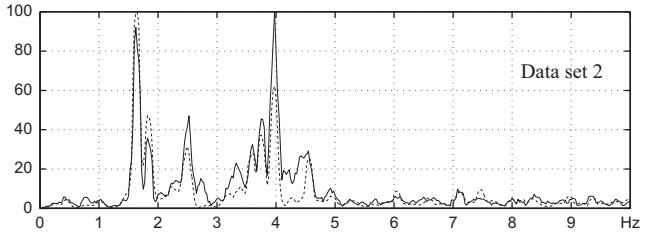

Fig. 10. Normalized power spectra of y_1; data-based (continuous line) and model-based (dashed line).

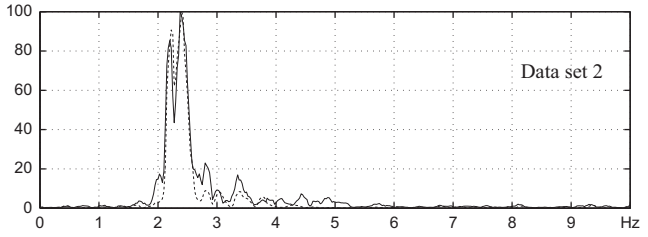

Fig. 11. Normalized power spectra of y_2; data-based (continuous line) and model-based (dashed line).

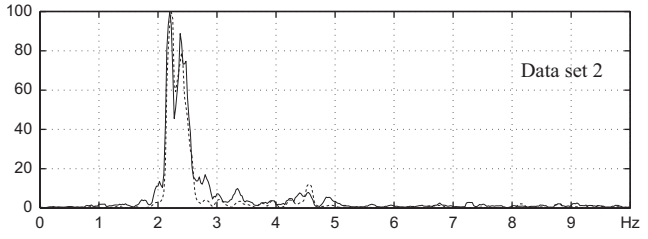

Fig. 12. Normalized power spectra of y_3; data-based (continuous line) and model-based (dashed line).

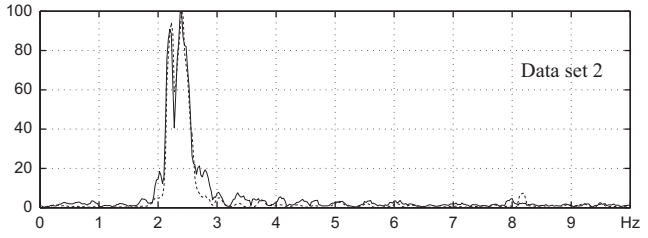

Fig. 13. Normalized power spectra of y_4; data-based (continuous line) and model-based (dashed line).

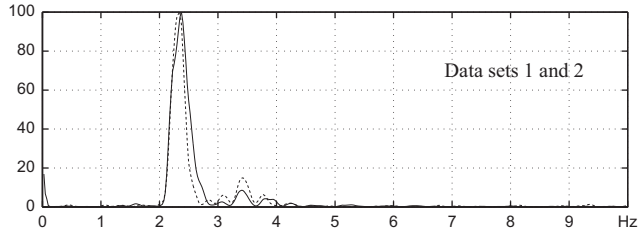

Fig. 14. Cross spectra between y_2 and y_1; model 1 (continuous line) and model 2 (dashed line).

is reported in Figs. 10–13. The associated significant peak frequencies, reported in Table 3, are congruent with those of the previous model. The cross-spectra between y_2 and y_1, y_3, y_4, computed with the models identified from the considered data sets, are reported in Figs. 14–16 that show good agreements. Similar results can be observed on remaining cross-spectra.

Please cite this article as: R. Guidorzi, et al., Structural monitoring of a tower by means of MEMS-based sensing and enhanced autoregressive models, European Journal of Control (2013), http://dx.doi.org/10.1016/j.ejcon.2013.06.004

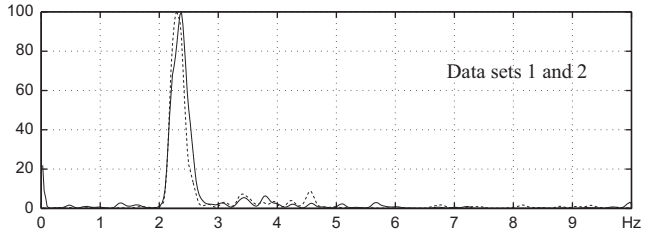

Fig. 15. Cross spectra between y_2 and y_3; model 1 (continuous line) and model 2 (dashed line).

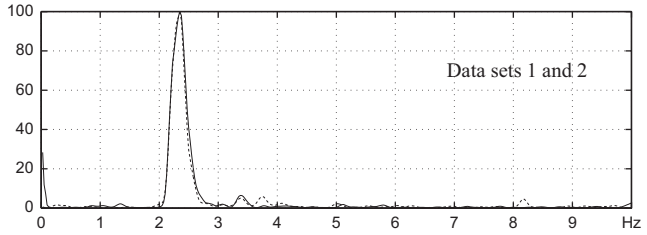

Fig. 16. Cross spectra between y_2 and y_4; model 1 (continuous line) and model 2 (dashed line).

A further check of the validity of the identified models has been performed by comparing their power spectra with those obtained with piezoelectric accelerometers placed in the same positions. Figs. 17 and 18 show that, even if the noise level of the MEMS-based sensing units is greater than that of piezoelectric accelerometers, the obtained PSDs are strongly congruent. This confirms the suitability of the identified models and of the SHM602 system for the performed task.

Finally, in order to confirm the good results obtained from the AR+noise model, a comparison with a classic frequency domain technique has been performed. The Enhanced Frequency Domain Decomposition (EFDD) technique is one of the most used identification techniques in civil engineering applications and it can be considered as an extension of the so-called Peak–Picking method. The modal parameters can be estimated from the output power spectral density (PSD), in the condition of white noise input and lightly damped structures. A Singular Value Decomposition (SVD) is carried out for the PSD matrix for each frequency and all modes contributing to the vibration information at a given frequency are separated into principal value and orthogonal vectors [4]. In the proximity of each PSD peak, the power of the measured signals can be attributed to a limited subset of modes. The first singular values correspond to these modes, while the other singular values that are not associated with any mode consist of decomposed noise contained in the signals. This means that the decomposition corresponds to a Single Degree of Freedom identification of the system for each singular value.

The singular value plot of the spectral density matrix concentrates information from all spectral density functions. Moreover, if the assumptions are fulfilled, this technique simply provides a modal decomposition of the vibration information, and the modal information for each mode – even in the case of closely spaced modes and noise – can be extracted easily and accurately, for example by means of the peak-picking method. Once that the natural frequencies have been identified by peak-picking, the mode shapes have been estimated by using the singular vector matrices and the equivalent single degree of freedom "spectral bells" are identified for each mode by comparing the estimated mode shape of interest with all vectors previously estimated throughout the spectrum by SVD of the PSD matrices. A comparison of the mode shapes is then carried out by computing the modal assurance criterion (MAC). All singular values corresponding to a MAC value

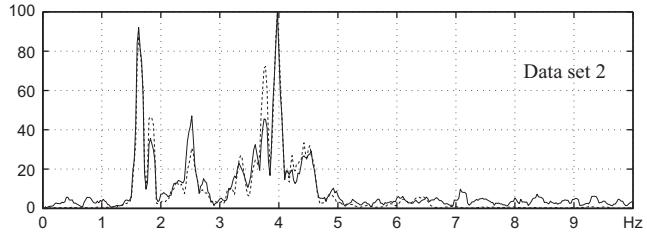

Fig. 17. Data-based PSD of y_1: data from MEMS (continuous line) and piezoelectric accelerometers (dashed line).

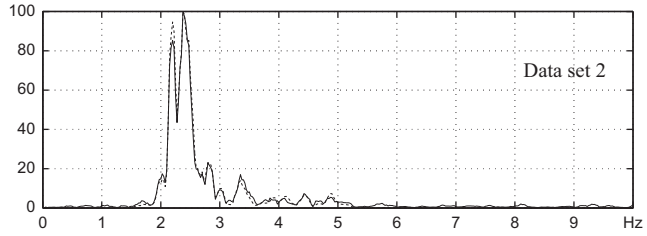

Fig. 18. Data-based PSD of y_2: data from MEMS (continuous line) and piezoelectric accelerometers (dashed line).

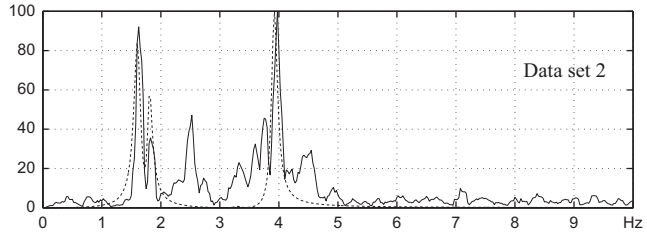

Fig. 19. Power spectra of y_1: data-based (continuous line) and obtained with the EFDD technique (dashed line).

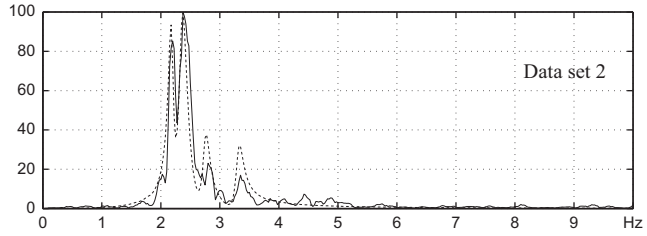

Fig. 20. Power spectra of y_2: data-based (continuous line) and obtained with the EFDD technique (dashed line).

superior to a user-specified parameter (which is called the MAC rejection level) are kept, thus forming an equivalent single degree of freedom spectral bell. Then, by inverse fast Fourier transform (IFFT) of that spectral bell, the resulting auto-correlation function can be used to reevaluate the frequency by counting the number of zero crossings in a finite time interval. Damping ratios are also estimated using the logarithmic decrement of the auto-correlation function [30].

After identifying the main modes, the PSD for each channel can be computed by means of the following equation:

$$\mathbf{P}_{yy}(j\omega) = \mathbf{G}(j\omega)^T \mathbf{P}_{xx}(j\omega)\mathbf{G}(j\omega) \tag{26}$$

where $\mathbf{P}_{xx}(j\omega)$ is the Power Spectra matrix of the inputs that is constant because the inputs are assumed as white noise processes

Please cite this article as: R. Guidorzi, et al., Structural monitoring of a tower by means of MEMS-based sensing and enhanced autoregressive models, European Journal of Control (2013), http://dx.doi.org/10.1016/j.ejcon.2013.06.004

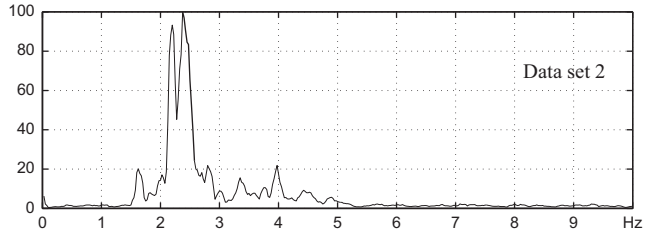

Fig. 21. EFDD technique: first singular value in the decomposed power spectra.

and $\mathbf{G}(j\omega)$ is the Frequency Response Function matrix. The Frequency Response Function $\mathbf{G}(j\omega)$ can be written, using a partial fraction expansion, in the following pole-residue form:

$$\mathbf{G}(j\omega) = \sum_{k=1}^{N} \left(\frac{R_k}{j\omega - \lambda_k} + \frac{\overline{R}_k}{j\omega - \overline{\lambda}_k} \right) \tag{27}$$

where the poles $\lambda_k = -\xi_k\omega_k + j\omega_k\sqrt{1-\xi_k^2}$ and the residues $R_k = \phi_k\gamma_k$ contain the identified parameters; "$\overline{\ }$" denotes the complex conjugate.

Figs. 19 and 20 report a comparison between the PSD of the recorded data and the estimated ones. It can be observed that the estimated PSD (dashed curves) does not always fit well the experimental ones. This is mainly due to a poor estimation of the damping ratios and to the fact that the selection of the eigenfrequencies can be a critical task (see, for example, Fig. 21).

5. Concluding remarks

This paper has described some families of multivariate models that can be used in SHM-oriented identification procedures and, in particular, the extension of AR models to consider the presence of additive measurement noise. It describes also the implementation, in the tower of the Engineering School of Bologna University, of a new advanced MEMS-based SHM system developed at Bologna University and engineered by Teleco. Two data sets collected by this system during small seismic events have been used to test the suitability for SHM applications of multivariate AR+noise models.

The congruence and effectiveness of the identified models have been verified by means of comparisons between the models obtained from different sets of data including the data obtained from temporarily installed seismic sensors.

The identified multivariate AR+noise models exhibit a strong congruence; a high level of congruence can also be observed between the power spectral densities of these models and those of the data used for their identification. The suitability of the new system for SHM applications has been verified by comparing the power spectral densities of the sequences obtained from this system with those of traditional (piezoelectric) accelerometers.

The conclusion that can be deduced from the tests is that MEMS-based systems can be as effective as traditional ones, despite the intrinsically higher level of noise, in SHM applications and that multivariate AR+noise models offer a useful tool for implementing modal-based SHM analyses.

References

[1] A.E. Aktan, F.N. Catbas, K.A. Grimmelsman, C.J. Tsikos, Issues in infrastructure health monitoring for management, Journal of Engineering Mechanics 126 (2000) 711–724.

[2] A. Bayraktar, A.C. Altunsik, B. Sevim, M.E. Kartal, T. Trker, Y. Bilici, Comparison of near and far fault ground motion effects on the nonlinear response of dam-reservoir-foundation systems, Nonlinear Dynamics 58 (2009) 655–673.

[3] A. Bonelli, O. Bursi, R. Ceravolo, S. Santini, N. Tondini, Dynamic identification and structural health monitoring of a twin deck curved cable-stayed footbridge: the "Ponte del Mare" of Pescara in Italy, in: Proceedings of the 5th European Conference on Structural Health Monitoring, Sorrento, Italy, 2010.

[4] R. Brincker, L. Zhang, P. Andersen, Modal identification of output-only systems using frequency domain decomposition, Smart Materials and Structures 10 (2001) 441–445.

[5] F.K. Chang (Ed.), in: Proceedings of the First, Second and Third International Workshops on Structural Health Monitoring, Stanford University, Stanford, CA, CRC Press, New York, 1997, 1999 and 2001.

[6] H.C. Chung, T. Enotomo, K. Loh, M. Shinozuka, Real-time visualization of bridge structural response through wireless MEMS sensors, in: Proceedings of SPIE—The International Society for Optical Engineering, 2004.

[7] R. Diversi, R. Guidorzi, U. Soverini, Identification of autoregressive models in the presence of additive noise, International Journal of Adaptive Control and Signal Processing 22 (2008) 465–481.

[8] R. Diversi, U. Soverini, R. Guidorzi, A new estimation approach for AR models in presence of noise, in: Preprints of the 16th IFAC World Congress, Prague, Czech Republic, 2005.

[9] S.W. Doebling, C.R. Farrar, M.B. Prime, D.W. Shevitz, A review of damage identification methods that examine changes in dynamic properties, Shock and Vibration Digest 30 (1998) 91–105.

[10] S.W. Doebling, C.R. Farrar, M.B. Prime, D.W. Shevitz, Damage Identification and Health Monitoring of Structural and Mechanical Systems from Changes in Their Vibration Characteristics: A Literature Review, Los Alamos National Laboratory Report LA-13070-MS, Los Alamos National Laboratory, Los Alamos, NM 87545, 1996.

[11] C.R. Farrar, S.W. Doebling, D.A. Nix, Vibration-based structural damage identification, Philosophical Transactions of the Royal Society: Mathematical, Physical & Engineering Sciences 359 (2001) 131–149.

[12] Fib Task Group 5.1, Monitoring and Safety Evaluation of Existing Concrete Structures, State-of-the-Art Report, Final Draft, 2002.

[13] Y. Fujino, A. Nishitani (Eds.), in: Proceedings of the Fifth World Conference on Structural Control and Monitoring (5WCSCM), Tokyo, 2010.

[14] Y. Gao, B.F. Spencer, Online damage diagnosis for civil infrastructure employing a flexibility-based approach, Smart Materials and Structures 15 (2006) 9–19.

[15] R. Guidorzi, Equivalence, invariance and dynamical system canonical modelling. Part I, Kybernetika 25 (1989) 233–257.

[16] R. Guidorzi, Equivalence, invariance and dynamical system canonical modelling. Part II, Kybernetika 25 (1989) 386–407.

[17] R. Guidorzi, Multivariable System Identification: From Observations to Models, Bononia University Press, Bologna, Italy, 2003.

[18] R. Guidorzi, R. Diversi, U. Soverini, The Frisch scheme in algebraic and dynamic identification problems, Kybernetika 44 (2008) 585–616.

[19] ISO/DIS 18649:2002(E). Mechanical Vibration—Evaluation of Measurement Results from Dynamic Tests and Investigations on Bridges, 2002.

[20] S.M. Kay, The effects of noise on the autoregressive spectral estimator, IEEE Transactions on Acoustics, Speech and Signal Processing 27 (1979) 478–485.

[21] S. Kim, Wireless Sensor Networks for Structural Health Monitoring, Master's Thesis, University of California at Berkeley, May 2005.

[22] H.S. Kim, H. Melhem, Damage detection of structures by wavelet analysis, Engineering Structures 26 (2004) 347–362.

[23] Q. Ling, Z. Tian, Y. Yin, Y. Li, Localized structural health monitoring using energy-efficient wireless sensor networks, IEEE Sensors Journal 9 (2009) 1596–1604.

[24] L. Ljung, System Identification—Theory for the User, Prentice Hall, Englewood Cliffs, NJ, 1999.

[25] J.P. Lynch, A. Sundararajan, K.H. Law, A.S. Kiremidjian, T. Kenny, E. Carryer, Embedment of structural monitoring algorithms in a wireless sensing unit, Structural Engineering and Mechanics 15 (2003) 285–297.

[26] C. Mazzotti, L. Vincenzi, Structural identification of a steel structure by forced vibrations, in: ICOSSAR—International Conference of Structural Safety and Reliability, Rome, Italy, 2005.

[27] A. Mita, T. Inamura, S. Yoshikawa, Structural health monitoring for buildings with automatic data management system, in: 4th International Conference on Earthquake Engineering, Taipei, Taiwan, 2006.

[28] T. Nagayama, B.F. Spencer, Structural Health Monitoring Using Smart Sensors, NSEL Report, Series 001, University of Illinois Urbana-Champaign, 2007 ⟨https://www.ideals.uiuc.edu/handle/2142/3521⟩.

[29] K.K. Nair, A.S. Kiremidjian, K.H. Law, Time series-based damage detection and localization algorithm with application to the ASCE benchmark structure, Journal of Sound and Vibration 291 (2006) 349–368.

[30] C. Rainieri, G. Fabbrocino, E. Cosenza, Structural health monitoring systems as a tool for seismic protection, in: Proceedings of the 14th World Conference on Earthquake Engineering, Beijing, China, 2008.

[31] F. Ricciardelli, A. Occhiuzzi, P. Clemente, Semi-active tuned mass damper control strategy for wind-excited structures, Journal of Wind Engineering and Industrial Aerodynamics 88 (2000) 57–74.

[32] M. Savoia, L. Vincenzi, Differential evolution algorithm for dynamic structural identification, Journal of Earthquake Engineering 12 (2008) 800–821.

[33] D. Skolnik, E. Yu, E. Taciroglu, J.W. Wallace, System identification and health monitoring studies on two buildings in Los Angeles, in: 6th International Workshop of Structural Health Monitoring, Stanford University, Stanford, CA, 2007.

[34] H. Sohn, C.R. Farrar, Damage diagnosis using time series analysis of vibration signals, Smart Materials and Structures 10 (2001) 446–451.

[35] Teleco SHM Systems site: ⟨www.telecoshmsystems.com⟩.

[36] L. Vincenzi, C. Mazzotti, M. Savoia, Modal identification of a TAV viaduct using subspace models, in: 2nd International FIB Congress, Naples, Italy, 2006.

Please cite this article as: R. Guidorzi, et al., Structural monitoring of a tower by means of MEMS-based sensing and enhanced autoregressive models, European Journal of Control (2013), http://dx.doi.org/10.1016/j.ejcon.2013.06.004

[37] Y. Wang, J.P. Lynch, K.H. Law, A wireless structural health monitoring system with multithreaded sensing devices: design and validation, Structure and Infrastructure Engineering 3 (2007) 103–120.
[38] K. Worden, C.R. Farrar, G. Manson, G. Park, The fundamental axioms of structural health monitoring, Proceedings of the Royal Society A 463 (2007) 1639–1664.
[39] G.J. Yuna, S.G. Lee, J. Carletta, T. Nagayama, Decentralized damage identification using wavelet signal analysis embedded on wireless smart sensors, Engineering Structures 33 (2011) 2162–2172.
[40] W.X. Zheng, A least-squares based method for autoregressive signals in the presence of noise, IEEE Transactions on Circuits and Systems—II 46 (1999) 81–85.
[41] W.X. Zheng, Fast identification of autoregressive signals from noisy observations, IEEE Transactions on Circuits and Systems—II 52 (2005) 43–48.

Please cite this article as: R. Guidorzi, et al., Structural monitoring of a tower by means of MEMS-based sensing and enhanced autoregressive models, European Journal of Control (2013), http://dx.doi.org/10.1016/j.ejcon.2013.06.004